Advanced Structured Materials

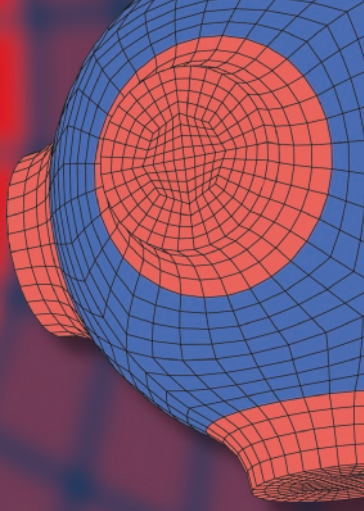

António Torres Marques
Sílvia Esteves
João P. T. Pereira
Luis Miguel Oliveira *Editors*

Additive Manufacturing Hybrid Processes for Composites Systems

Springer

Advanced Structured Materials

Volume 129

Common engineering materials reach in many applications their limits and new developments are required to fulfil increasing demands on engineering materials. The performance of materials can be increased by combining different materials to achieve better properties than a single constituent or by shaping the material or constituents in a specific structure. The interaction between material and structure may arise on different length scales, such as micro-, meso- or macroscale, and offers possible applications in quite diverse fields.

This book series addresses the fundamental relationship between materials and their structure on the overall properties (e.g. mechanical, thermal, chemical or magnetic etc.) and applications.

The topics of *Advanced Structured Materials* include but are not limited to

- classical fibre-reinforced composites (e.g. glass, carbon or Aramid reinforced plastics)
- metal matrix composites (MMCs)
- micro porous composites
- micro channel materials
- multilayered materials
- cellular materials (e.g., metallic or polymer foams, sponges, hollow sphere structures)
- porous materials
- truss structures
- nanocomposite materials
- biomaterials
- nanoporous metals
- concrete
- coated materials
- smart materials

Advanced Structured Materials is indexed in Google Scholar and Scopus.

More information about this series at http://www.springer.com/series/8611

António Torres Marques · Sílvia Esteves ·
João P. T. Pereira · Luis Miguel Oliveira
Editors

Additive Manufacturing Hybrid Processes for Composites Systems

Springer

Editors
António Torres Marques
Department of Mechanical Engineering
Faculty of Engineering
University of Porto
Porto, Portugal

Sílvia Esteves
Product and Systems Development
INEGI—Institute of Science and Innovation
in Mechanical and Industrial Engineering
Porto, Portugal

João P. T. Pereira
Product and Systems Development
INEGI—Institute of Science and Innovation
in Mechanical and Industrial Engineering
Porto, Portugal

Luis Miguel Oliveira
Product and Systems Development
INEGI—Institute of Science and Innovation
in Mechanical and Industrial Engineering
Porto, Portugal

ISSN 1869-8433 ISSN 1869-8441 (electronic)
Advanced Structured Materials
ISBN 978-3-030-44521-8 ISBN 978-3-030-44522-5 (eBook)
https://doi.org/10.1007/978-3-030-44522-5

This Springer imprint is published by the registered company Springer Nature Switzerland AG
The registered company address is: Gewerbestrasse 11, 6330 Cham, Switzerland

Preface

This book is centred on the emergent technology of additive manufacturing (AM) and its application beyond the state of the art in fibre reinforcement thermoplastics (FRTP). It includes the development of a hybrid and integrated process that combines, into a single-step platform, additive and subtractive operations and allows CAD-to-Part productions with freeform shapes using long or continuous FRTP. Moreover, it addresses the following engineering issues:

- Design rules for hybrid additive manufacturing (hAM).
- Thermoplastics compounds for AM processing appropriate to high temperature and strength applications.
- Advanced extrusion heads and process concepts for AM of FRTP.
- Hybridization strategies regarding AM specifications (supports, slicing, filling, etc.) and material in-process properties (rheology, interfacial adhesion, layer consolidation, etc.).
- Software ecosystem for hAM design, pre-processing, process planning, emulating and multi-axis processing.
- Three-dimensional path generator for hAM based on a multi-objective optimization algorithm that matches the recent curved adaptive slicing method with a new transversal scheme.
- hAM parameters real-time monitoring and closed-loop control.
- Multi-parametric nondestructive testing (NDT) tool customized for FRTP AM parts.
- Sustainable manufacturing process validated by advanced LCA/LCC models.

Development of a constitutive model to predict the elasto-plastic behaviour of 3D-Printed thermoplastics using a meshless formulation. Covering the whole value chain, this next-generation technology is presented starting with part design, simulation and materials composition; then going through transformation stages; and finishing with the product evaluation and end-of-life studies.

Additive manufacturing (AM) is one of the most promising manufacturing technologies nowadays. Aeronautics and aerospace surrendered to the advantages of AM. The sale of AM professional industrial equipment increased regularly and is

expected the worldwide turnover on AM to quadruple between 2015 and 2020. Numbers are even more impressive for metal additive manufacturing showing the higher growth rates within the different available additive technologies.

Similarly, the composite materials industry assists a movement of great progression and penetration into new sectors, exploring the main advantages of high performance allied to lightweight designs. In order to reduce the labour intensive and manual operations typically associated with composite fabrication and to satisfy the needs for flexible automated composite processes, research is committed in investigating the feasibility of highly automated, integrated and reproductive processes based in principles such as extrusion, automated tape placement or automated fibre placement.

Several scientific initiatives are known to intent the implementation of composite manufacturing processes through AM, but these attempts collide with a number of shortcomings that limit their usability. Identified issues are related to the layer-by-layer approach of AM without reinforcements between layers (composites anisotropy that decreases through-thickness properties), the use of short fibres, the high roughness low-quality surface finishing, the added complexity of algorithms and motion paths. The poor performance of raw materials when directly used in AM processes without appropriate properties optimization and the dependence on experimental equipment based on available commercial machines (mainly SLS and FDM) without proper design for the processes to be implemented is also an important issue.

Still, there are insufficient or no exploration of certain required scientific fields starting by the balancing of properties when composing raw materials for AM processes. The fabrication of the fibre-reinforced composite filaments or laminates is required as a pre-step before AM processing, necessitating the need for materials to be composed and developed. A fibre-reinforced thermoplastic raw material for AM proposes should present an adequate rheological profile (viscosity), compatibility with the heat sources (softening/melting temperature ranges) and suitable mechanical behaviour in terms of ductility and flexibility avoiding brittleness. Using long or continuous fibres instead of short fibres is difficult to incorporate into processing and additional processing functions have to be merged like the fibre cutting systems.

The purpose of this book is to walk through the challenging scientific route to develop an advanced hybrid additive manufacturing process beyond the state of the art, which enables the lightweight design and manufacture of fibre-reinforced thermoplastics products under ecological friendly conditions.

The research developments presented in this book include a high potential manufacture process, the additive manufacturing hybridized with subtractive technologies and an innovative product and high-performance composite parts produced without moulds and with tailored properties. Both process and products hold a high potential of, in future, converting into tradable goods fostering the industry in particular and the economy in general.

The authors acknowledge the funding received by Project POCI-01-0145-FEDER-016414—FIBR3D, co-financed by COMPETE 2020 and LISBOA 2020, through Fundo Europeu de Desenvolvimento Regional (FEDER) and by National Funds through Fundação para a Ciência e Tecnologia (FCT).

Porto, Portugal

António Torres Marques
Sílvia Esteves
João P. T. Pereira
Luis Miguel Oliveira

Contents

Acronyms

3D	Three Dimensions
ABS	Acrylonitrile butadiene styrene
AM	Additive manufacturing
AR	Aramidic fibre
ASTM	American Society for Testing and Materials
ATC	Automatic trajectory control
ATRP	Atom transfer radical polymerization
BiCGStab	Bi-conjugated gradient stabilized
CAD	Computer-aided design
CAM	Computer-aided manufacturing
CBAM	Composite-based additive manufacturing
CCD	Charge-coupled device
CFD	Computational fluid dynamics
cFR	Continuous fibre reinforced
CFRP	Carbon fibre-reinforced polymer
cFRTP	Continuous fibre-reinforced thermoplastics
CIRP	College International pour la Recherche en Productique
CLFDM	Curved Layered Fused Deposition Modelling
CMOS	Complementary metal-oxide semiconductor
CNC	Computer numeric control
CNT	Carbon nanotube
DCB	Double cantilever beam
DED	Direct energy deposition
DFM	Design for manufacturing
DfMA	Design for additive manufacturing
DIC	Diagonal incomplete-Cholesky
DILU	Diagonal incomplete-LU
DIY	Do-it-yourself
DMA	Dynamic mechanical analysis
DMD	Direct metal deposition

DOE	Design of experiments
DSC	Differential scanning calorimetry
EBM	Electron beam melting
EC	Eddy current
EHS	Experimental hybrid system
EM	Electromagnetism-like
EPDs	Environmental report declarations
ER	Experimental rig
ERS	Experimental rig system
FBG	Fibre Bragg gratings
FDM	Fused deposition modelling
FEA	Finite element analysis
FEM	Finite element modelling
FFF	Fused filament fabrication
FGM	Functionally graded materials
FP	Fabry–Perot
FRTP	Fibre-reinforced thermoplastics
G-Code	G-code protocol (ISO/DIN 66025 standard)
GnP	Graphene nanoplatelets
GS	Granty speed
HVAC	Heating, ventilation and air conditioning
IPC	Institute of Polymers and Composites
IR	Infrared
ISO	International Organization for Standardization
L/C-FRTP	Long and continuous fibre-reinforced thermoplastics
LC	Life cycle
LCA	Life cycle assessment
LCC	Life cycle cost
LENS	Laser Engineering Net Shape
LM	Layer-by-layer manufacturing
LMD	Laser metal deposition
MAT	Medial axis transformation
MEMS	Microelectromechanical system
MFG	Multi-functional and graded features
MFI	Melt Flow Index
MIP	Mathematical integer programming
MIT	Massachusetts Institute of Technology
MMC	Metal matrix composites
MOPSO	Multi-objective particle swarm optimization
MQ	Multi-quadric
MT	Magnetic particle testing
MWCNT	Multi-walled carbon nanotube
NASA	National Aeronautics and Space Administration
NDT	Nondestructive testing
NiTi	Nitinol

NPV	Net present value
NSGA-II	Non-dominated sorting genetic algorithm
OCT	Optical coherent tomography
OEM	Original equipment manufacturer
OM	Origami mechanism
PA	Polyamide
PA 12	Polyamide 12
PA 66	Polyamide 66
PAEK	Polyaryletherketone
PAI	Polyamide-imide
PBF	Powder bed fusion
PC	Polycarbonate
PCG	Pre-conditioned conjugate gradient
PCL	Polycaprolactone
PCR	Product Category Rules
PDMS	Poly (dimethylsiloxane)
PE	Polyester
PEEK	Polyetheretherketone
PEI	Polyetherimide
PEKK	Poly Ether Ketone Ketone
PES	Polyethersulphone
PI	Polyimide
PLA	Polylactic acid
PMMA	Polymethyl methacrylate
POF	Polymeric optical fibres
PPPA	Phenylphosphonic acid
PPS	Polyphenylene sulphide
PPSU	Polyphenylsulphone
PS	Polystyrene
PT	Penetrant testing
PTFE	Polytetrafluorethylene
PVC	Polyvinyl chloride
R&D	Research and development
RA	Raster angle
RBF	Radial basis function
RP	Rapid prototype
RPIM	Radial point interpolation method
RTM	Resin transfer moulding
RVE	Representative volume element
SAFE	Semi-analytical finite element method
sCF	Short carbon fibres
sCFPA12	Short carbon fibre polyamide 12
SEM	Scanning electron microscopy
SETAC	Society for Environmental Toxicology and Chemistry
sFRTP	Short fibre-reinforced thermoplastics

SHS	Selective heat sintering
SLA	Stereolithography (Chap. 2)
S-LCA	Social life cycle assessment
SLE	Selective laser erosion
SLM	Selective laser melting
SLS	Selective laser sintering
SMA	Shape memory alloys
SMP	Shape memory polymers
SROI	Social return on investment
STL	Stereolithography (Chap. 1)
STL	Standard Tessellation Language (Chap. 2)
TGA	Thermogravimetric analysis
TMA	Thermomechanical analysis
TO	Topology optimization
TPO	Thermoplastic olefin
TW	Welding time
UAV	Unmanned aerial vehicle
UD	Unidirectional
UNEP	United Nations Environmental Programme
US	Ultrasound
UT	Ultrasonic tests
UTS	Ultimate tensile strength
VE	Vinylester
WLF	Williams–Landel–Ferry
Xc	Degree of crystallinity

Symbols and Units

ρ	Density
γ'	Shear rate
$\emptyset$	Diameter
$\varphi_j(\boldsymbol{x}_\mathrm{I})$	Interpolations functions (Chap. 6)
$\varphi^\mathrm{T}(\boldsymbol{x}_\mathrm{I}) = \{\varphi_1(\boldsymbol{x}_\mathrm{I}), \varphi_2(\boldsymbol{x}_\mathrm{I}), \ldots, \varphi_n(\boldsymbol{x}_\mathrm{I})\}$	Interpolation function calculated at the interest point
$\boldsymbol{\sigma}$	Stress tensor (Chap. 6)
$\sigma_\mathrm{Y}\vert_\mathrm{tensile}, \sigma_\mathrm{Y}\vert_\mathrm{comp}$	Yield stresses of the same material when subjected to tensile or compression loads, respectively (Chap. 6)
$\boldsymbol{\varepsilon}$	Strain tensor (Chap. 6)
$\delta\boldsymbol{\varepsilon}$	Virtual strain tensor (Chap. 6)
$\delta\boldsymbol{u}$	Virtual displacement (Chap. 6)
$d\lambda$	Plastic strain multiplier (Chap. 6)
$\mathrm{d}\boldsymbol{\varepsilon}^\mathrm{e}$	Infinitesimal elastic strain increments (Chap. 6)
$\mathrm{d}\boldsymbol{\varepsilon}^\mathrm{p}$	Infinitesimal plastic strain increments (Chap. 6)
$\mathrm{d}\boldsymbol{\sigma}$	Stress increment (Chap. 6)
$\boldsymbol{\sigma}_{\mathrm{Y}0}$	Initial yield stress (Chap. 6)
λ	Relaxation time
τ	Deviatoric stress tensor
$\square$	E-step values
∇	Gradient
Ω	Domain (Chap. 6)
Γ	Boundary (Chap. 6)
$\boldsymbol{a}$	Normal vector (Chap. 6)
$a_i(\boldsymbol{x}_\mathrm{I}), b_j(\boldsymbol{x}_\mathrm{I})$	Non-constant coefficients of $R_i(\boldsymbol{x}_\mathrm{I})$ and $p_j(\boldsymbol{x}_\mathrm{I})$, the polynomial basis, respectively, with m being the basis monomial number (Chap. 6)

a_T	Shift factor
A	Hardening parameter (Chap. 6)
$\boldsymbol{b}$	Body forces per unit volume (Chap. 6)
$\boldsymbol{B}$	Deformation matrix (Chap. 6)
BT	Building time
c, p	Shape parameters (Chap. 6)
c_1	WLF parameter
c_2	WLF parameter
cm	Centimetre
c_p	Heat capacity
°C	Degree Celsius
°C/min	Degree Celsius per minute
$\boldsymbol{D}_{ep}$	Elasto-plastic constitutive matrix given (Chap. 6)
ΔH_f0	Standard enthalpy of formation
ΔH_m	Melting enthalpy
$\Delta\lambda_{FBG}$	FBG wavelength shift
$\Delta\lambda_{FP}$	FP wavelength shift
$\Delta\varepsilon$	Strain shift
ΔT	Temperature shift
Δt	Periods of time
f	Frequency
F, G and H	Material constants and characterize the anisotropy (Chap. 6)
g/10 min	Gram per ten minutes
$\boldsymbol{G}$	Matrix (Chap. 6)
G′	Storage modulus
G″	Loss modulus
GPa	Gigapascal
h	Hour
h	Convection coefficient
H'	Proportionality parameter used to update the yield stress based on strain hardening (Chap. 6)
$\boldsymbol{H}$	Blocks of diagonal matrixes, $\boldsymbol{H}^j$, containing the shape function of each node j of a given 'influence domain', with $\boldsymbol{H}^j = \varphi_j(\boldsymbol{x}_I)\boldsymbol{I}$ (Chap. 6)
H_c	Enthalpy of combustion
Hz	Hertz
i	Node calculated at the interest point $\boldsymbol{x}_I$ (Chap. 6)
I	Period

$\boldsymbol{I}$	Identity matrix with dimension $[d \times d]$, where d is the number of degrees of freedom of the analysed problem (Chap. 6)
J	Joule
J/g	Joule per gram
k	Thermal conductivity
$k_{\mathrm{FBG}\varepsilon}$	Strain sensitivity
k_{FBGT}	Temperature sensitivity
kg	Kilogram
kg/h	Kilogram per hour
kN	Kilonewton
$\boldsymbol{K}_0$	Initial stiffness calculated using the elastic constitutive matrix, $\boldsymbol{D}$ (Chap. 6)
$\boldsymbol{L}$	Differential operator (Chap. 6)
L_0	Length of filament at the pre-set extruder speed
L_{arb}	Arbitrary Length
L_{real}	Real Length
L_{ref}	Reference mark on the filament
L_{rem}	Remaining Length
µm	Micrometre
m	Mass
m	Metre
m/min	Metre per minute
mg	Milligram
mL/min	Millilitre per minute
mm	Millimetre
mm/s	Millimetre per second
$\dot{M}_i$	Throughput
MPa	Megapascal
n	Power law exponent
n	Number of nodes within the 'influence domain' of $\boldsymbol{x}_{\mathrm{I}}$ (Chap. 6)
η^*	Complex viscosity
η_∞	Viscosity at the lower Newtonian plateau
η_0	Viscosity at the upper Newtonian plateau
N	Newton
p	Pressure
$\boldsymbol{p}$	Polynomial matrix (Chap. 6)
Pa	Pascal
Pa s	Pascal second
$\boldsymbol{R}$	Matrix (Chap. 6)
Ra	Surface roughness measure
$R_i(\boldsymbol{x}_{\mathrm{I}})$	Radial basis function RBF (Chap. 6)
rpm	Revolution per minute

s	Second
SA	Support area measure
SE	Staircase effect measure
SA	Adapted support area measure
SE	Adapted staircase effect measure
t	Time
$\bar{\boldsymbol{t}}$	Traction forces acting on the natural boundary Γ_{t} (Chap. 6)
t_1, t_2	Initial and final time (Chap. 6)
T	Temperature
T_0	Reference temperature
T_{c}	Crystallization temperature
T_{g}	Glass transition temperature
T_{m}	Melting temperature
u	Velocity vector
$\boldsymbol{u}$	Displacement field (Chap. 6)
$\boldsymbol{u}$	Kinematically admissible displacement field (Chap. 6)
$\boldsymbol{u}_i$	Value of the field variable in the node i and $\varphi_i(\boldsymbol{x}_{\mathrm{I}})$ (Chap. 6)
$\dot{\boldsymbol{u}}$	Velocity (Chap. 6)
$\boldsymbol{u}(\boldsymbol{x}_{\mathrm{I}}) = \sum_{i=1}^{n} \varphi_i(\boldsymbol{x}_{\mathrm{I}})\, \boldsymbol{u}_i$	Interpolation functions, being n the number of nodes inside the 'influence domain' of the interest point $\boldsymbol{x}_{\mathrm{I}}$ (Chap. 6)
v_{ext}	Pre-set extruder speed
V	Volt
$\boldsymbol{x}_{\mathrm{I}}$	Integration point (Chap. 6)
$\boldsymbol{x}_{\mathrm{I}}, \boldsymbol{x}_{\mathrm{J}}$	Interest points containing the same number of nodes (sixteen), but a different radius ($\mathrm{r_I} \neq \mathrm{r_J}$) (Chap. 6)
W	Relative water content
W/g	Watt per gram
W/m K	Watt per metre Kelvin

Chapter 1
State-of-the-Art Review and Roadmap

Isaac Ferreira, Margarida Machado, Elsa Henriques, Marco Leite, Paulo Peças, and António Torres Marques

Abstract This chapter is devoted to the study of the key principles of AM value chain, including materials (in particular fibre-reinforced thermoplastics—FRTP), pre-processing, process and control aspects, design features, quality and robustness issues, applications and sustainability concerns. It will label the technological challenges involved and outline the potential of applicability of a roadmap. After starting with materials, processes and applications mapping, we will address new strategies for AM FRTP parts performance improvement. Then, FRTP parts certification and quality assurance will be discussed and a LCA/LCC analysis of composite materials is presented. Finally, a AM and composites research roadmap is proposed.

Keywords Additive manufacturing · Hybrid manufacturing · Fused deposition modelling · Quality assurance · LCA/LCC · Fibre-reinforced thermoplastics

I. Ferreira (✉) · M. Machado · A. T. Marques
INEGI—Institute of Science and Innovation in Mechanical and Industrial Engineering, FEUP Campus, Rua Dr. Roberto Frias, 400, Porto, Portugal
e-mail: iaferreira@inegi.up.pt

M. Machado
e-mail: mmachado@inegi.up.pt

A. T. Marques
e-mail: marques@fe.up.pt

E. Henriques · M. Leite · P. Peças
Instituto Superior Técnico, Avenida Rovisco Pais 1, 1049-001 Lisboa, Portugal
e-mail: elsa.h@tecnico.ulisboa.pt

M. Leite
e-mail: marcoleite@tecnico.ulisboa.pt

P. Peças
e-mail: ppecas@tecnico.ulisboa.pt

A. Torres Marques et al. (eds.), *Additive Manufacturing Hybrid Processes for Composites Systems*, Advanced Structured Materials 129,
https://doi.org/10.1007/978-3-030-44522-5_1

1.1 Materials, Processes and Applications Mapping

1.1.1 Scientific Status

1.1.1.1 Polymer Nanocomposites

Polymer nanocomposites consist of a polymer matrix reinforced with filler(s) that have at least one dimension smaller than 100 nm and that exhibit a significantly better performance than the matrix at low filler loadings. Polymer nanocomposites have caught the attention of the industrial and scientific communities due to their potential for developing novel, cost-effective and high-performance materials for advanced engineering applications, namely where high thermal and electrical conductivity are necessary. Electrically conductive nanocomposites are quite interesting for fused filament fabrication (FFF) applications, providing that they fulfil the requirements of the process and the necessary functionalities.

Percolation theory predicts that there is a critical conductive filler concentration at which composites with insulating matrices become electrically conductive. This concentration defines the electrical percolation threshold and strongly depends on the aspect ratio (length/diameter), agglomerate density and strength, purity and/or surface modification, alignment of carbon nanoparticles, and on the polymer type and nanoparticle dispersion. The research carried out so far on composites with carbon nanoparticles has shown that lower percolation concentrations and higher electrical conductivity levels are typically achieved in composites with carbon nanotubes (CNT) compared to composites with graphene derivatives. Hence, the use of hybrid filler systems combining CNT with graphite, exfoliated graphite or graphite nanoplates, has been explored [1–4].

Effective dispersion of carbon nanoparticles in polymeric matrices remains a critical issue that has hindered their application, while requiring the incorporation of higher percentages of filler than those that would be anticipated [5]. In the pristine state, carbon nanoparticles tend to form clusters with strong cohesive forces. In addition, the chemical inertia due to the lack of chemical functionalities presented by these nanoparticles precludes their prospect to establish strong interfaces with polymer molecules. Thus, surface modification of carbon nanoparticles and compatibilization with the polymer matrix is sometimes desired, although its effect on the nanoparticle dispersion is still not completely clear.

In practice, three main approaches for polymer nanocomposites preparation: (i) in situ polymerization of monomers in the presence of the nanoparticles; (ii) a dissolution of the polymer in a solvent followed by mixing and dispersion of the nanoparticles; and (iii) melt mixing of a thermoplastic polymer with the carbon nanoparticles, using batch or continuous mixing equipment [6]. In situ polymerization and solution-based techniques rely on the capacity of a low viscous medium to intercalate the particles. Although they are expected to achieve high dispersion levels, they are oriented to laboratory scale and batch production. Additionally, they require

the use of solvents and catalysts, which may compromise the purity of the final nanocomposites [7].

Melt mixing attempts to create sufficiently high hydrodynamic stresses. It utilizes conventional polymer compounding technologies (e.g. twin-screw extrusion, batch mixers, micro-compounders) and is less environmentally aggressive. However, this is a complex process composed of many parameters; hence, it is not easy to establish clear correlations between material characteristics, processing conditions and final dispersion levels. For example, the creation of high thermomechanical stresses might be useful for dispersion but may simultaneously induce the thermal degradation of the matrix.

The nature of the carbon nanoparticles and polymers chosen to form a composite strongly influences the dispersion process and thus the electrical properties of the composite [8, 9]. The polymer melt viscosity plays also a crucial role on the kinetic and mechanism of carbon nanoparticle dispersion. The dispersion mechanisms (rupture versus erosion) of particles in non-Newtonian fluids postulated by Manas-Zloczower et al. [10, 11] are mainly dependent on the fragmentation number, which is directly proportional to flow viscosity and shear rate and inversely proportional to agglomerate cohesive strength.

The latter can be significantly reduced after polymer chain infiltration, which seems to be faster when agglomerates are less densely packed and polymer melts have lower viscosity [12]. Since the viscosity of polymers depends on shear rate, molecular weight distribution and temperature, the infiltration process can be affected considerably by processing conditions (mixing speed, throughput or residence time) and raw materials selection. Despite lower melt viscosity facilitating agglomerate infiltration, the shear stresses applied to the agglomerates are also lower, resulting in lower Fa and lower probability for the rupture mechanism to take place [12, 13].

The stability of the morphology of nanocomposites containing CNTs or graphene nanoplatelets (GnPs) when submitted to an additional thermomechanical cycle has also been investigated [14–16]. The question has practical relevance in the context of FFF, since the manufacture and the processing of the material into a final product are carried out in separate thermal cycles. Nanocomposites containing 2 or 10 wt% of graphite nanoplates were prepared by melt mixing using a small-scale intensive mixer coupled to a capillary rheometer [14]. Regardless of filler loading, a significant decrease of the agglomerate size took place in the first part of the mixer, as the material is subjected to a combination of shear and extensional stresses. In the intermediate chamber, where the shear rate is very low, a significant increase of the agglomerate area occurred, suggesting that re-agglomeration took place. Interestingly, the morphology and/or cohesion of these re-formed agglomerates seemed to be different from that of the initial agglomerates, affecting its subsequent dispersion rate in the second mixing zone, as well as the final conductivity. It was also found that surface modification of GnP with the polymer enhanced the stability of the dispersion and delayed re-agglomeration.

It should also be stressed that the manufacture, extrusion and additive manufacturing of polymer nanocomposites can be successfully performed by melt mixing. However, the high viscosities and high transition temperatures required by some

advanced materials such as polyamide-imide (PAI), polyaryletherketone (PAEK), polyetheretherketone (PEEK), polyetherimide (PEI) polyethersulphone (PES), polyimide (PI) or polyphenylsulphone (PPSU) demand processing equipment capable to withstand higher temperatures, higher torques and higher abrasion resistance.

Cicala et al. [17] focused on exploring the potential of PEEK filaments as novel FFF material and comparing their mechanical properties with those of commercially available filaments. It is reported that FFF-printed PEEK has excellent mechanical properties; however, printing defects are often present, and that further research is necessary with respect to the process optimization, essentially in decreasing pore formation during the printing process. Vaezi and Yang [18, 19] reported a successful low-cost 3D printing of PEEK structures using filament-based extrusion AM process. Compression, tensile and three-point flexural tests were performed to study the mechanical properties of these new 3D printed PEEK structures. Davies et al. [20] investigated the properties of PEEK-CNT composite filaments in order to understand required parameterization for layer-by-layer material deposition. The resulting composites showed that temperature does not affect the significantly the tensile strength of the composite. The authors claimed that the presence of CNTs seems to influence more the processing behaviour rather than the reinforcing performance.

Jia et al. [21] developed a new kind of PA6-based filament with good toughness for FFF via a facile method, adding maleic anhydride grafted poly (ethylene 1-octene) and polystyrene (PS) into polyamide 6 (PA6) matrix, which disturb the crystallization, reduce the shrinkage stress and help the shape stability of the printed products.

1.1.1.2 Continuous Fibre-Reinforced Thermoplastics

Long and continuous fibre-reinforced thermoplastics (L/C-FRTP) present improved properties and could replace conventional thermoset matrix composites in numerous markets. Their major advantages are: excellent toughness, durability and damping properties, easier storage, reshaping, reparability and more favourable recycling and processing routes which do not involve chemical reactions [22]. However, the difficulty in impregnating and wetting continuous fibres with high-viscosity thermoplastics composites remains a major obstacle to the application of continuous FRTPs. Thus, in the latest years, several research and development (R&D) works have been carried out to develop more efficient ways of impregnating fibres with high-viscosity thermoplastics and overpass this major problem. The main techniques studied involve: (i) the thermoplastic melting, (ii) the decreasing of thermoplastic viscosity and (iii) the intimate fibre/matrix contact prior to final impregnation [23, 24].

1.1.1.3 Impregnation of Continuous Fibres with Thermoplastics

Techniques involving the polymer viscosity decreasing only can be used with few thermoplastics, which must present low molecular weight stages/precursors or being

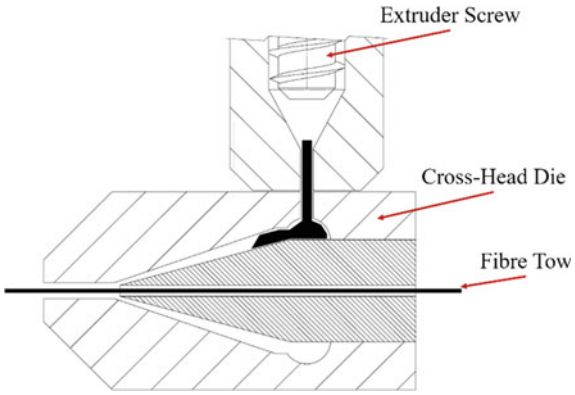

Fig. 1.1 Cross-head extrusion die

easily dissolved in solvents. This may imply toxicity and explosion hazards or presence of voids generated during solvent removal. On the other hand, intimate fibre/matrix contact processes involve always the use of second final impregnation stage, where pressure and temperature must be applied, to allow the continuous fibres to be totally embedded into the thermoplastic matrix. Thus, a direct melting process where the continuous fibre strand/tow is pulled passing through a cross-head extrusion die (Fig. 1.1), being achieved the full impregnation of the continuous fibres. The fully impregnated continuous fibre-reinforced thermoplastic tape obtained can be wound in a spool for being used in the additive manufacturing machine.

If considered advantageous, intimate fibre/matrix techniques may be also used as alternative. Such techniques do not lead to immediate fibre impregnation but bring the polymer and fibres to such a close proximity that impregnation can be easily done through the minimized polymer flow, which the application of pressure and heat may generate during processing. In such case, either unidirectional continuous fibre-reinforced thermoplastic matrix towpregs (Fig. 1.2a) or commingled fibres (Fig. 1.2b) may be used. In both cases, any of these products must be made to pass through a heated die to obtain a fully impregnated tape. This can be done previously to or during the additive manufacturing fabrication.

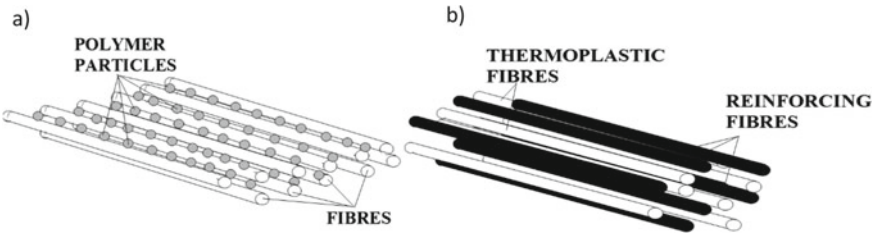

Fig. 1.2 Intimate continuous fibre/matrix products

Towpregs (Fig. 1.2a) consist on a continuous fibre strand/tow dry-coated with small drops of a thermoplastic matrix and can be produced by using a prototype patented machine that exists in the Institute of Polymers and Composites (IPC) laboratories [25]. Commingled fibres (Fig. 1.2b) are fibre strand mixing unidirectional reinforcing fibres with thermoplastic extruded ones that may be also produced in our laboratories. In this case, both types of fibres are placed in very close proximity in order to minimize the flow distance necessary to achieve full impregnation during squeezing under heat.

1.1.1.4 Filament Interface Wettability

Products made by FFF can vary significantly in quality, depending on operation parameters, machine specifications, material properties and part geometry [26]. The quality, evaluated in terms of surface finish, dimensional accuracy and mechanical strength, is influenced by the evolution with time of filament temperature during deposition [27–29] controlling the construction of the part and the adequacy of the bonding between contiguous filament segments [26].

The formation of the bonding in the FFF process is driven by the thermal energy of the semi-molten material. The FFF prototypes are orthotropic composites of polymer filaments partial bonding between filaments, and voids (Fig. 1.3) [27–29].

The quality of the bond formed between individual filaments depends on the growth of the neck formed between adjacent filaments (wetting) and on the molecular diffusion and randomization at the interface. The bond formation process can be modelled following approaches similar to those used to describe polymer welding, where the issue of molecular diffusion dominates. It can also be assumed as a sintering process for which the wetting phenomenon is also of importance. At the macro-level,

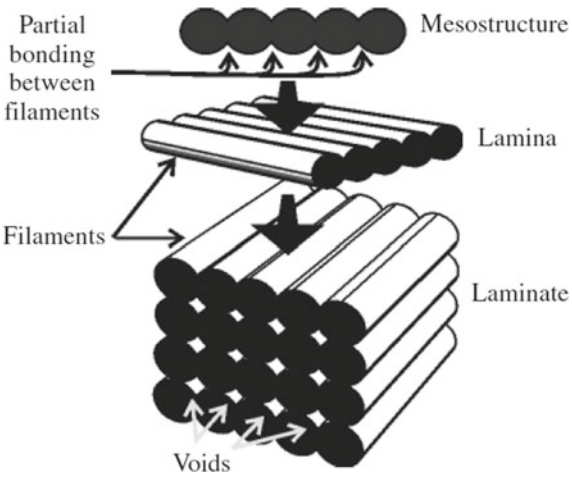

Fig. 1.3 Levels of analysis for FFF prototypes [27, 29]

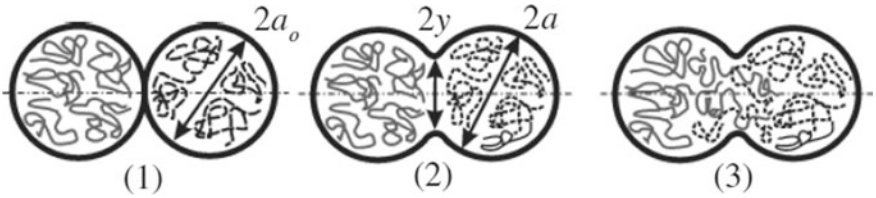

Fig. 1.4 Bond formation process between two Filaments: (1) surface contacting, (2) neck growth, (3) diffusion at interface and the final randomization [29]

the properties are studied as laminates of bonded laminas (Fig. 1.3). At the micro-level, the properties of each lamina are functions of the properties of the filaments, the quality of the bonds between filaments, and void density [27, 29].

In this work, Céline et al. [27] estimated the dynamics of bond formation from sintering data of acrylonitrile butadiene styrene (ABS) filaments. According to this, the formation of bonds between polymer filaments in the FFF process can be described as shown in Fig. 1.4. The first step of the process is the establishment of interfacial molecular contact by wetting. The molecules then undergo motions towards preferred configurations to achieve the adsorptive equilibrium [30, 31]. Molecules diffuse across the interface, forming an interfacial zone, and/or react to form primary chemical bonds across the interface. The randomization can be reached only after extensive interdiffusion of chain segments under critical conditions. The dimensionless sintering neck growth is calculated as the ratio of neck radius y with the filament's radius a, as indicated in Fig. 1.4 [27].

Sun et al. [29] and Gurrala et al. [28] analyzed changes in the mesostructure and degree of healing at the interfaces between adjacent polymer filaments. They concluded that fabrication strategy, environment temperature and variations in convection determine the overall quality of the bond strength.

Bellini et al. [32, 33] used ANSYS POLYFLOW to model the extrusion, deposition and cooling stages of FFF, taking into consideration heat exchanges with the surroundings, between filament segments and between filament and support. Bonding was predicted using a wetting-diffusion model based on the reptation theory and it was shown that lower cooling rates promote stronger bonding. The temperature predictions were validated experimentally.

Yardimci and Güçeri [34] and Yardimci et al. [30] modelled the cooling of a filament due to convection with the environment (i.e. disregarding contacts with adjacent segments) and showed the effect of adopting different build strategies.

Costa et al. [35] examined the contribution of various thermal phenomena during FFF to the overall heat transfer, including convection and radiation with the environment, conduction with support and between adjacent filament segments, radiation between adjacent filament segments and convection with entrapped air. It was demonstrated that during the deposition step, heat exchanges by convection with the environment, by conduction between adjacent filament segments and by conduction with the support are relevant in terms of temperature evolution. It was also shown